



ZÁPADOČESKÁ
UNIVERZITA
V PLZNI

Vaclav Skala
University of West Bohemia
Plzen, Czech Republic
www.VaclavSkala.eu

Rongjiang Pan
Shandong University
Jinan, China
panrj@sdu.edu.cn

Ondrej Nedved
University of West Bohemia
Plzen, Czech Republic
onedved@kiv.zcu.cz



Simple 3D Surface Reconstruction Using Flatbed Scanner and 3D Print

1. Introduction

Reconstruction of nearly flat 3D objects can be used in many applications, e.g. getting 3D surface for games, reconstruction of historical fragments etc. The presented approach uses a flatbed scanner to reconstruct a surface of nearly flat objects without calibration and produce a 3D copy of the scanned object using a 3D printer.

Position of the light source and CCD sensor in 2D flatbed scanners is not generally the same, i.e. the sensor is aligned with $-z$ axis and the light is coming under some angle α . That causes small "shadowed" contours in scanned images. The given object is scanned in four orthogonal positions and the four scanned images are aligned.

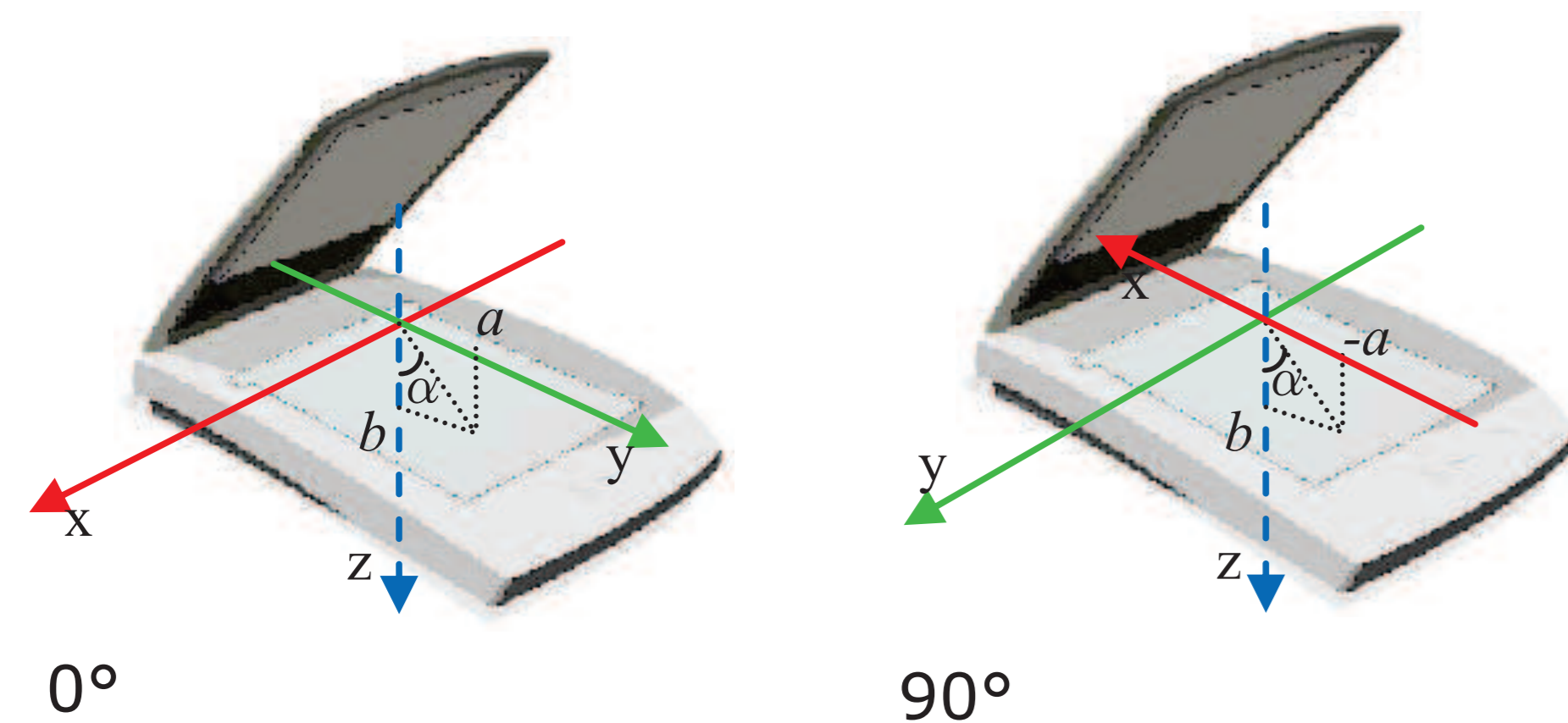


Figure 1: Two of four fundamental orientations in scanning.

2. Normal Vector Reconstruction

The CCD sensor of the flatbed scanner is aligned vertically and the light source is fixed under α angle. Therefore it is possible to reconstruct normal vector \mathbf{n} for each point on the surface as the scanned pixel's intensity I_0 is given as:

$$I_0 = \rho \int_{-l}^l \langle \mathbf{n}, \mathbf{l} \rangle dx = \rho(n_y a + n_z b) \int_{-l}^l \frac{1}{\sqrt{x^2 + a^2 + b^2}} dx = \rho s(n_y a + n_z b)$$

where: $\mathbf{l} = [x, a, b]^T / \sqrt{x^2 + a^2 + b^2}$ is the normalized lighting vector and

$$s = \int_{-l}^l \frac{1}{\sqrt{x^2 + a^2 + b^2}} dx = 2 \ln \frac{l + \sqrt{l^2 + a^2 + b^2}}{\sqrt{a^2 + b^2}}$$

Similarly it can be computed for other positions. This leads to equations:

$$\begin{bmatrix} 0 & \tan \alpha & 1 \\ 0 & -\tan \alpha & 1 \\ -\tan \alpha & 0 & 1 \\ \tan \alpha & 0 & 1 \end{bmatrix} \begin{bmatrix} \rho s b n_x \\ \rho s b n_y \\ \rho s b n_z \end{bmatrix} = \begin{bmatrix} I_0 \\ I_{180} \\ I_{90} \\ I_{270} \end{bmatrix}$$

Solved with least squares error approach we get:

$$\begin{aligned} \rho s b n_x &= \frac{I_{270} - I_{90}}{2 \tan \alpha} & \rho s b n_y &= \frac{I_0 - I_{180}}{2 \tan \alpha} \\ \rho s b n_x &= \frac{I_0 + I_{180} + I_{90} + I_{270}}{4} & \tan \alpha &= \frac{a}{b} \end{aligned}$$

A curvature optimization can also be made to obtain better results. However the crucial step is the surface reconstruction from the obtained map of normal's and boundary conditions, actually height on the object boundary.

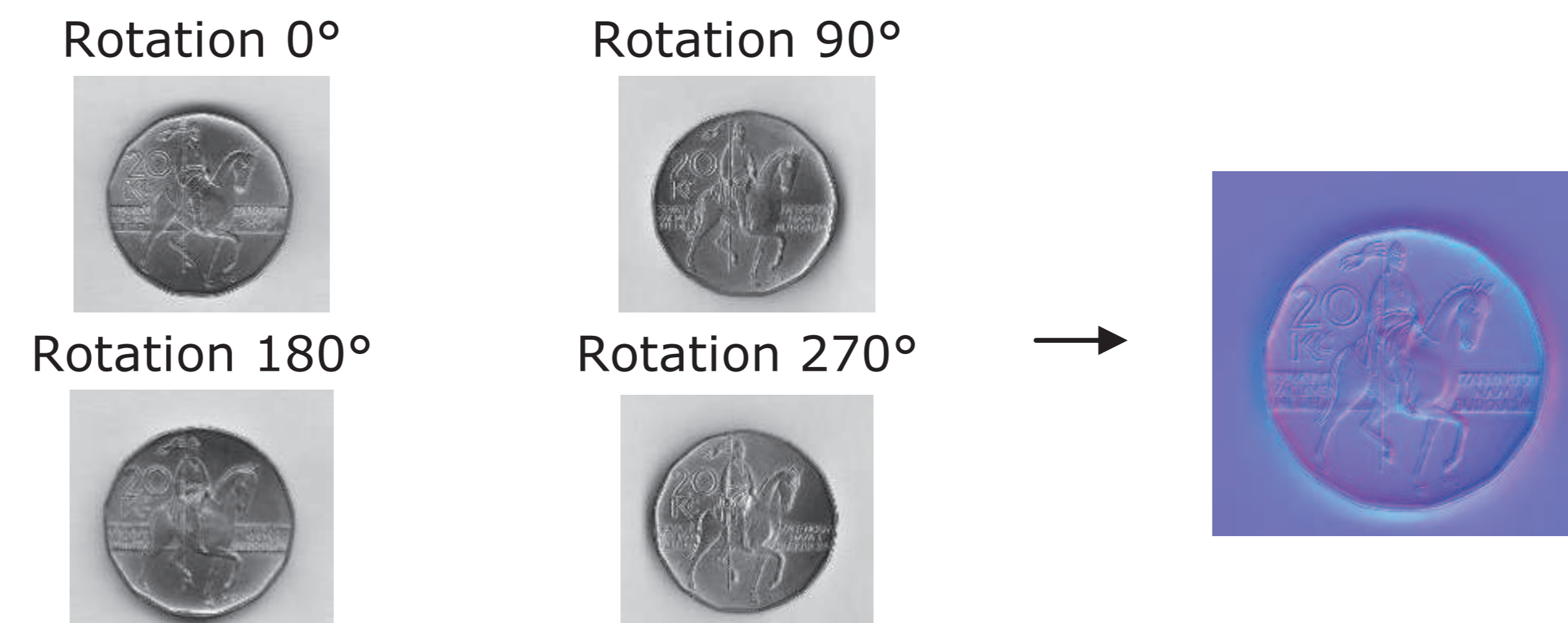


Figure 2: Four scans reconstructed into a normal map.

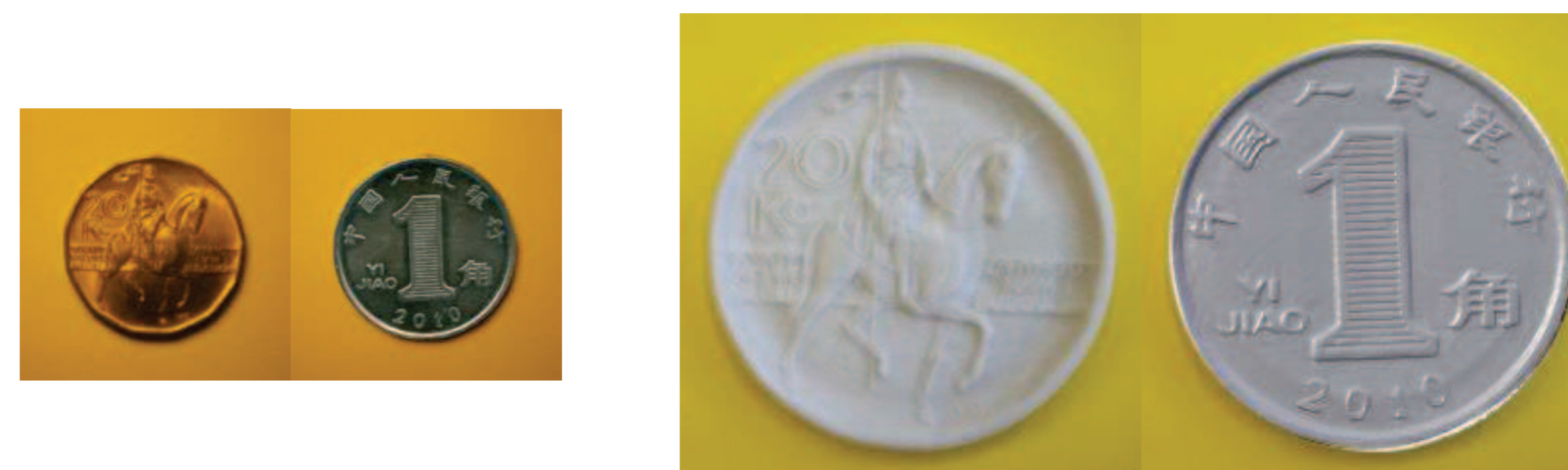


Figure 3: Original object and reconstructed surface.

3. Surface Reconstruction

As we expect nearly flat 3D objects, known height on a boundary is assumed. The inner part, i.e. 3D profile, is given by the normal vector reconstruction part. It means that it is a "classical" 2D boundary problem known from Finite Elements Methods, which leads to solution of a sparse linear system of equations $\mathbf{Ax} = \mathbf{b}$ in general. However, the normal reconstruction process is still very noisy. Therefore for the reconstruction two orthogonal 1D reconstructions were used, i.e. for x and y axes. This leads to over-determined linear system of equations, therefore least square error was used for solution. When a surface is reconstructed, a triangular mesh is generated so that the volume is closed and thus ready for the 3D print. In Fig.2, the scanned coin was of a diameter of 25 mm. The reconstructed object was scaled to a diameter of 55mm since the 3D printer's grain we used is 0.1 mm.

4. Implementation

A software solution including both, the normal's reconstruction and the surface integration was implemented. As for the limitations of the object to be scanned, it is possible to process any smooth surface up

to the depth of 1 mm to 2 mm. The finest details of deeper objects begin to fade due to the constant focus of the optical system of the scanner. Considering size limitations, any relevant input object resulting in a model printable on the ZPrinter® 650 is acceptable.

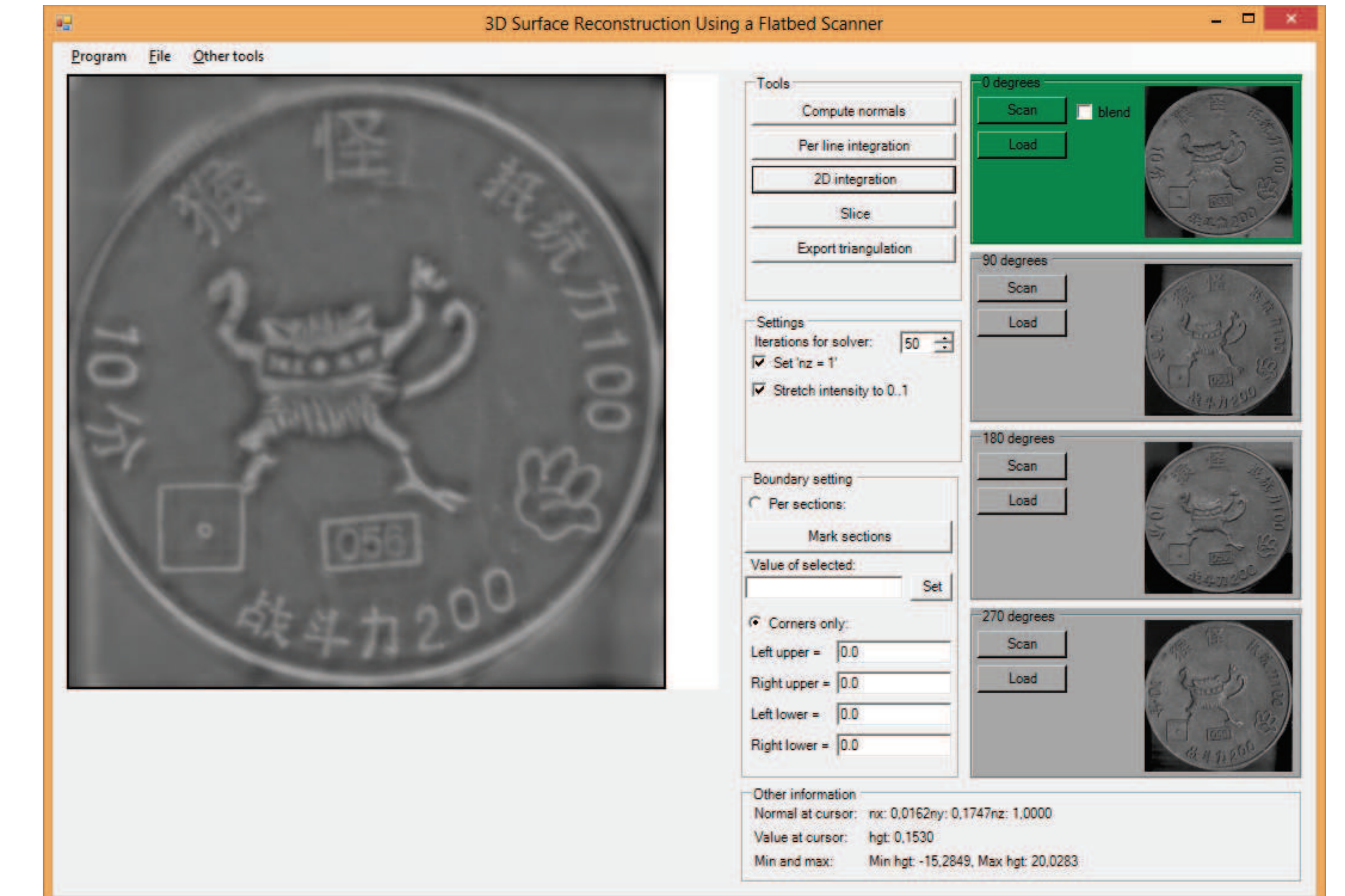


Figure 4: User's interface.

5. Conclusion

The presented concept was experimentally verified and 3D reconstructed objects were printed on a 3D printer. It should be noted that some 2D scanners may produce images with a small deformation due to an improper motion of the head of the scanner which should be accordingly corrected to get better results.

References

- [1] Brown,B., Toler-Franklin,C., Nehab, D, Burns,M., Dobkin,D., Vlachopoulos,A., Dumas,C., Rusinkiewicz,S., Weyric,T. 2008. A system for high-volume acquisition and matching of fresco fragments: Reassembling Theran wallpaintings. ACM Trans.Graph., pp.1-9.
- [2] Clarkson,W., Weyrich,T., Finkelstein,A., Heninger,N., Halderman,J.A., Felten,E.W. 2009. Finger printing Blank Paper Using Commodity Scanners. In IEEE Symp. on Security and Privacy (SP '09). IEEE Comp. So., Washington, USA, 301-314.
- [3] Johnson,M.K., Cole,F., Raj,A., Adelson,E.H. 2011. Microgeometry capture using an elastomeric sensor. ACM TOG 30, No.4, Article 46.
- [4] Martedi,S., Saito,H., Sevieres,M. 2009. 3D Shape Reconstruction of Sole Surface of Human Foot using Flatbed Scanner, FCV 2009.
- [5] Pintus,R., Malzbender,T., Wang,O., Bergman,R., Nachlieli,H., Ruckenstein,G. 2010. Photo Repair and 3D Structure from Flatbed Scanners Using 4- and 2-Source Photometric Stereo. Computer Vision, Imaging and Computer Graphics. Theory and Applications, Springer Berlin Heidelberg, Vol.68, pp.326-342.
- [6] Woodham,R.J. 1980. Photometric Method for Determining Surface Orientation from Multiple Images. Optical Eng., 19(1):139-144.
- [7] Pan,R., Skala,V. 2013. Normal Map Acquisition of Nearly Flat Objects Using a Flatbed Scanner, accepted, 3VR conference ICVRV 2013 - Xian, China